ELSEVIER

Journal of Nuclear Materials 290–293 (2001) 1018–1022

journal of nuclear materials

www.elsevier.nl/locate/jnucmat

Mitigation of plasma–wall interaction during quasi-single helicity states in RFX

G. Spizzo [a,b,c,*], P. Franz [a,b], L. Marrelli [a], P. Martin [a,b,d], A. Murari [a], T. Bolzonella [a], D. Terranova [a,b,c], P. Zanca [a]

[a] *Consorzio RFX, Associazone EURATOM–ENEA sulla Fusione, Corso Stati Uniti 4, Padova 35127, Italy*
[b] *Istituto Nazionale Fisica della Materia, UdR Padova, Italy*
[c] *Dipartimento di Ingegneria Elettrica, Università di Padova, Padova, Italy*
[d] *Dipartimento di Fisica, Università di Padova, Padova, Italy*

Abstract

The paper presents new results, obtained in the RFX device, about MHD mode locking in the reversed field pinch. The differences in the mode locking phenomenology between multiple helicity (MH) and quasi-single helicity (QSH) states are discussed, in particular as far as the plasma–wall interaction and the total radiation emission are concerned.

Keywords: Radiation; Emission asymmetry; Reversed field pitch; RFX; Quasi-single helicity states

1. Locked modes in the reversed field pinch

When a relatively large number of $m = 0$ and $m = 1$ MHD modes are simultaneously destabilised in the reversed field pinch (RFP) configuration, they tend to lock in phase producing a toroidally localised distortion of the magnetic equilibrium. Phase-locked modes (LM) have in fact been observed in several RFP experiments [1–3] and in particular also in RFX [4,5], the large European experiment where the measurements discussed in this paper have been taken. In RFX, the effect of LM is worsened since they also lock to the wall, in one particular toroidal location, throughout the discharge. This produces a severe plasma–wall interaction (PWI), which in some cases can become intolerable [5].

The search for effective recipes to mitigate or, even better, avoid the negative effects of LM has been a key issue in the RFX experimental activity [6].

In this paper, we report new magnetic and total radiation results which show how the PWI induced by LM has been reduced by accessing a novel experimental regime, i.e., the quasi-single helicity (QSH) regime. Total radiation measurements have been obtained with a bolometric tomographic diagnostic [7], which has already allowed the characterisation of total radiation emissivity profiles in the unperturbed region of the plasma [8].

2. Phase locking in MH and QSH states

2.1. The shape of the locked mode as deduced from magnetic measurements

In the standard case, the k spectrum of the $m = 1$ modes is rather broad: many modes with sizeable amplitudes and different n's are simultaneously present in the plasma [9]. This situation corresponds to the multiple helicity (MH) state. Recent experiments and theoretical studies [10] have shown that there is an important bifurcation in the RFP dynamics: the plasma can in fact access a so called QSH state, where the n-spectrum of $m = 1$ modes is dominated by an individual ($m = 1$, $n = n_0$) mode. In this case, the core plasma assumes a helical topology. When the growth of the dominant mode is concomitant with a reduction of the other $m = 1$

* Corresponding author. Tel.: +39-049 829 5975; fax: +39-049 870 0718.
E-mail address: spizzo@igi.pd.cnr.it (G. Spizzo).

0022-3115/01/$ - see front matter
PII: S0022-3115(00)00462-1

modes (the so-called 'secondary' modes), a significant increase of the global plasma confinement is observed. This is the case, for example, of pulsed poloidal current drive (PPCD) and oscillating poloidal current drive (OPCD) experiments [10].

To illustrate this point, Fig. 1 describes a plasma where MH and QSH regimes alternate. Fig. 1(A) shows the time evolution of the amplitudes of the toroidal component of the $m = 1$ magnetic modes, with various n's, measured with pick-up probes at the internal thick shell radius. We note that at $t \sim 0.04$ s the plasma moves to a QSH state: the $(m = 1,\ n = 7)$ mode suddenly increases and the secondary modes decrease. This phase lasts till $t \sim 0.06$ s, when the dominant mode decreases and this is associated with the increase of the other n's. As a result the k spectrum broadens. The absolute, non-axisymmetric displacement Δ of the last closed flux surface (LCFS) in MH conditions, reconstructed from magnetic measurements [11], is reported in Fig. 1(D) versus the toroidal angle ϕ measured along the torus major circumference. As expected, a broad spectrum of Fourier modes in the k space corresponds to a narrow perturbation in the real space. Typically, this perturbation spans approximately an angle $\Delta\phi \sim 40°$; it produces a localised PWI, whose typical signature is a significant local increase of the total radiation emissivity, which in some cases can reach extremely high values (up to 100 MW/m^3) [12]. Fig. 1(E) shows the horizontal component, Δ_H, of Δ.

In principle, if we had a pure SH state as those predicted by numerical simulations [13], the all plasma would assume a helical shape, and the LCFS would have a helical distortion. The maximum displacement of the LCFS would be therefore constant as a function of the toroidal angle ϕ and indeed there would be no localised perturbation at all. Actually, in real QSH cases, we do not obtain a pure SH state and the secondary modes have non-zero amplitude. Nonetheless, the maximum displacement Δ_{max} changes significantly in QSH states. This is shown in Fig. 1(B): the $\Delta(\phi)$ function does not show a pronounced maximum and it is more uniform, oscillating around a pedestal due to the helical distortion associated to the dominant $m = 1$ mode. The existence of a dominant $n = 7$ modulation is evident in the Δ_H trace, shown in Fig. 1(C). When, as during PPCD, the onset of a QSH state is associated to a significant decrease of the global mode amplitude, an even lower amplitude of the $\Delta(\phi)$ function is recorded and it approaches more closely the theoretical prediction, as shown in Fig. 2.

The rather different shape of the $\Delta(\phi)$ function in QSH states with respect to MH states is found also on a statistical basis. Fig. 3 shows the standard deviation of the $\Delta(\phi)$ function, normalised to its mean value, $\tilde{\Delta}(\phi)/\langle\Delta(\phi)\rangle$, versus the spectral spread number, N_s. Following [14], N_s is defined as

$$N_s = \left[\sum_n \left(\frac{W_{n\phi}}{\sum_n W_{n\phi}}\right)^2\right]^{-1},$$

where $W_{n,\phi}$ is the energy of the $(m = 1, n)$ mode. N_s is an indicator of the number of n modes composing the spectrum, and as N_s approaches unity the n spectrum narrows. We observe that $\tilde{\Delta}(\phi)/\langle\Delta(\phi)\rangle$ decreases as the plasma gets closer to a pure SH state. Given the typical

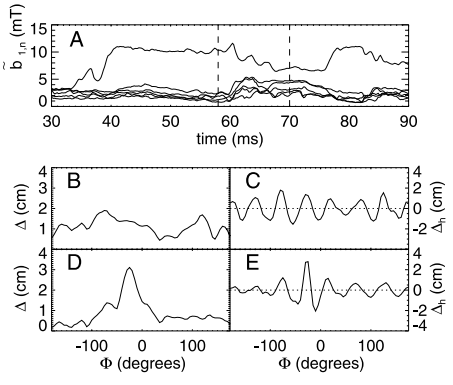

Fig. 1. (A) Temporal evolution of the magnetic spectrum for shot #13128, an example of spontaneous back-transition from QSH to MH states. The bold line corresponds to the dominant $m = 1, n = 8$ mode. (B–D) Plasma LCFS total displacement Δ and (C–E) its horizontal component Δ_H in function of the toroidal angle ϕ for $t = 58$ ms (B, C, a QSH state) and $t = 70$ ms (D, E, an MH state).

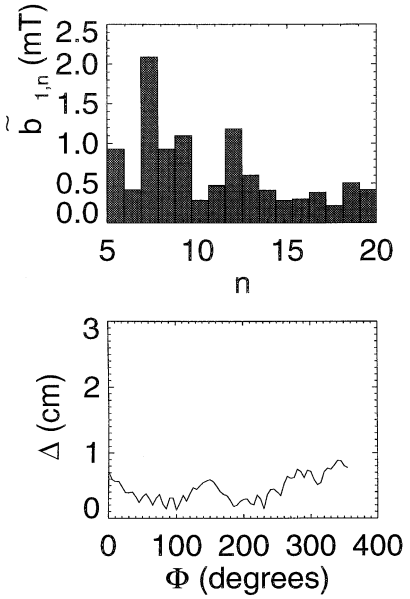

Fig. 2. Magnetic k spectrum and LCFS total displacement Δ for a QSH state with a low level of secondary modes (PPCD experiment).

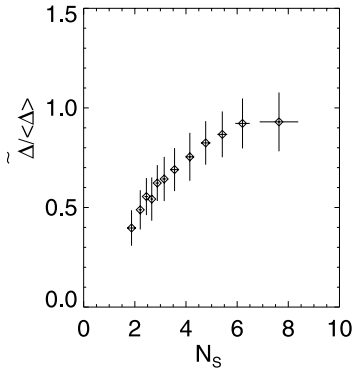

Fig. 3. Standard deviation of the $\Delta(\phi)$ function, normalised to the mean value, $\tilde{\Delta}(\phi)/\langle\Delta(\phi)\rangle$ in function of the spectral spread N_s.

shapes of the $\Delta(\phi)$ function described in Fig. 1, this indicates that a more uniform $\Delta(\phi)$ is present in QSH conditions. No pronounced localised structures are therefore present as $N_s \to 1$.

2.2. Relationship between locked mode and local radiation

The situation in MH states has been greatly improved with the successful active control of tearing mode rotation [15]. With this technique, we have induced a controlled rotation of the localised magnetic perturbation induced by the LM, thus spreading the interaction over the whole first wall and not only in a particular toroidal location. In Fig. 4(A), the scattered

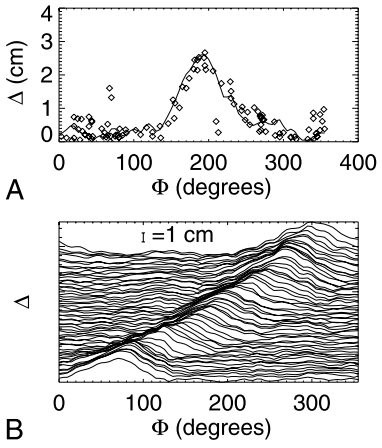

Fig. 4. (A) Reconstructed form of the locked mode during mode rotation: scattered points represent measurements of the local magnetic shift at different times, at the tomography location, whereas the solid line represents a reconstruction of the plasma displacement when the perturbation is just in front of the tomography (shot #13067); (B) time evolution of the $\Delta(\phi)$ profile.

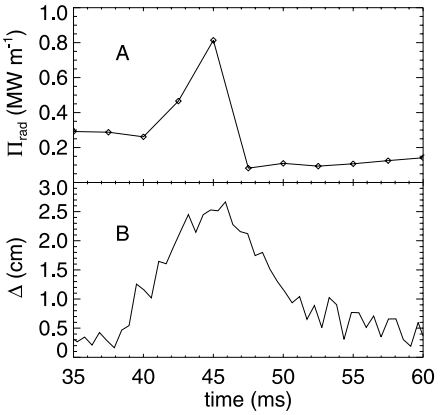

Fig. 5. Tearing modes active control experiments. (A) Time evolution of the linear power density Π_{rad} measured at the tomography location ($\phi = 202°$) and (B) of Δ at the same toroidal angle.

points are the local plasma displacements measured at the tomography location ($\phi = 202°$) at different times, whereas the solid line is the reconstruction of the plasma LCFS when the LM is just in front of the tomography. Fig. 4(B) shows the time evolution of the whole $\Delta(\phi)$ function. We deduce that, even if the perturbation does not rotate rigidly, since the phase relation between the modes changes in time, the shape of the LM is locally maintained.

The increased radiative emission can thus be related to the local magnetic shift. For this purpose, we define the linear power density Π_{rad} as the poloidal integral of the emissivity, following [12]. The results of these comparisons are summarised in Fig. 5. We note the perturbation travelling in the toroidal direction, together with the associated radiation burst caused by the enhanced PWI in correspondence of the rotating LM. The increase of the total radiation, is correlated to the displacement caused by the LM, which brings the magnetic field lines to intercept the first wall.

3. Total radiation profiles in QSH states

3.1. Radiation profiles in MH and QSH states

If the total radiation is linked to the extent of the magnetic deformation in the LM region, then one expects a difference in the plasma radiative behaviour between MH and QSH states. As a result of the mitigation of the LM in the QSH states, we measure significative changes in the total radiation emissivity profiles. Fig. 6 shows the total radiation emissivity profiles in three conditions. Scattered points are the line-integrated total radiation measurements ('brightness'), as detected by the

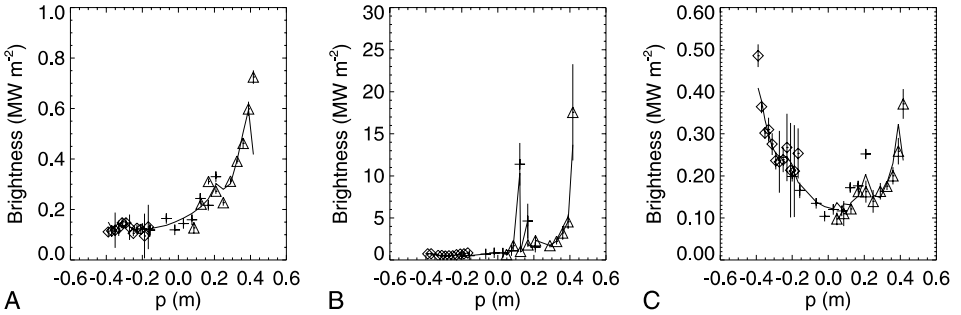

Fig. 6. Measured brightness and total radiation emissivity profiles in (A) a MH plasma, far from the LM region; (B) in a MH plasma, in the LM region and (C) a QSH plasma, far from the locked mode, with a low level of secondary modes (PPCD experiments).

bolometer array, while the solid line is the tomographic reconstruction of plasma emissivity. The abscissas are the chord impact parameters p, as defined in [8]. Each profile can be thus viewed as a horizontal slice of plasma emission.

Cases (A) and (B) refer to an MH discharge, but in the former the profile measurement is taken far from the LM region, whereas in the latter just in the LM region. Case (C) refers to a QSH state with a very low level of secondary mode energy. All of the discharges shown have the same value of plasma current ($I \sim 800$ kA) and of I/N value ($\approx 2 \times 10^{-14}$ Am), where N is the cross-section integrated density. In the standard MH state, far from the LM region, the profile is shifted outward, thus following the Shafranov shift (as discussed in [8]). In the MH–LM region, the profile is highly asymmetric in poloidal direction, and bursts in the radiation are observed, corresponding to highly localized interaction of the plasma with the first wall, as measured by CCD cameras [16]. This is related to the strong bulging caused by the LM. In the QSH state, with a low level of secondary mode activity, the overall radiation is lower, and the profile is more regular. These measurements, indicate that the PWI is on the average more distributed along the toroidal circumference. In fact, in the MH state we have two distinct toroidal regions: one in the proximity of the LM (~40° wide with a bursty emissivity like that of Fig. 6(B)) and the other covering the rest of the column. Here there is a poloidally asymmetric profile almost constant in the toroidal direction. In the QSH, when the whole plasma column assume a helical distortion, the bolometric emissivity profiles reflect an analogous helical behaviour. In fact, the in–out asymmetry (here defined as in [12]) of the brightness profile varies according to the horizontal component of the plasma local shift, due to the aforementioned helical perturbation, as shown in Fig. 7. For example, Fig. 6(C) corresponds to a plasma where the dominant mode points inward at $\phi = 202°$.

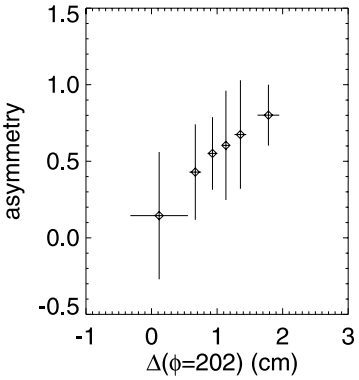

Fig. 7. Profile asymmetry in function of the local displacement Δ for a wide number of QSH and MH discharges. Same shot ensemble of Fig. 2.

3.2. Profile time evolution during bursty QSH states

The general picture described up to now is consistent with data, but it is worth mentioning that the detailed behaviour of plasma emissivity in QSH states depends on several factors, like precise width of the spectrum, the relative phases between the modes, the wall conditioning, the density, etc. Among these factors, the relative amplitude of the secondary modes with respect to the dominant one is important, in particular when their amplitude is not very small as in the PPCD cases. For example, Fig. 8 shows a quantitative evaluation of the changes in total radiation emissivity in the LM region during a spontaneous QSH helium discharge, where significant oscillations of the amplitude of the secondary modes with respect to the dominant one are observed. These oscillations lead to periodic broadening of the $m = 1$ spectrum, measured by the periodic increase of N_s. In this case, there are no longer radiative spots, as in hydrogen discharges (see Fig. 6(B) as an example), and the radiative mantle is thicker. When N_s increases, i.e., the QSH is weaker, the total radiated power density Π_{rad}

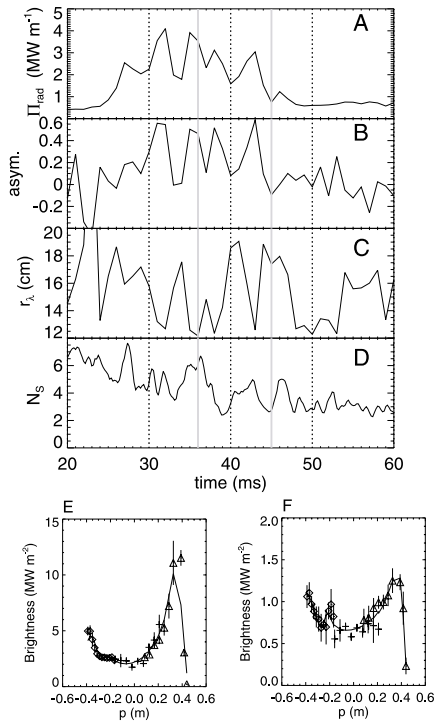

Fig. 8. Top: time evolution of (A) emitted power density Π_{rad}, (B) profile asymmetry, (C) radial extension of the emitting layer, r_λ, and (D) spectral spread number N_s for shot #10889. Bottom: two reconstructions corresponding to the coloured bars, in a MH (E) and QSH (F) state. The shot is performed in helium, thus the wide extension of the emitting layer.

increases, the profile asymmetry increases as well, and the layer thickness diminishes. Reconstructions of the total radiation emissivity, performed via a hybrid method [8], show the changes in the profile for two fixed times. It is worth noting that the cyclic changes in the radiation, due to the dominant mode fluctuations, are no longer present when the secondary mode energy decreases. This can be explained observing that there is a residual displacement due to the more or less coherent superposition of the secondary modes, that plays a role in determining the total radiation behaviour.

4. Summary and conclusions

In this paper, a comparison between the radiation properties in MH and QSH states has been discussed. In MH states we find that the only way to reduce the strong emission related to PWI, already discussed in [12], is the application of a technique to induce controlled rotation of the LM. The shape of the LM depends on three basic factors: (1) the energy of the dominant mode, (2) the energy of the secondary modes and (3) the relative phase between them. The increased radiation in the LM region is linked to the increased magnetic displacement, and thus can be reduced controlling MHD activity. When the plasma accesses QSH states, where the level of magnetic stochasticity inside the plasma is reduced, we record significant changes of the emissivity profiles, which hints that the radiation emission from the plasma edge is globally more symmetric. This likely means a more gentle and uniform PWI interaction in QSH states with respect to MH states.

Acknowledgements

The authors acknowledge the RFX team for the continuous support in the experimental activity.

References

[1] T. Tamano et al., Phys. Rev. Lett 59 (1987) 1444.
[2] A. Almagri et al., Phys. Fluids B 4 (1992) 4080.
[3] Y. Yagi et al., Phys. Plasmas 6 (1999) 3824.
[4] G. Rostagni, Fus. Eng. Design 25 (1995) 301.
[5] M. Valisa et al., J. Nucl. Mater. 241–243 (1997) 988.
[6] M. Valisa et al., these Proceedings.
[7] P. Martin, A. Murari et al., Rev. Sci. Instrum. 68 (1997) 1256.
[8] L. Marrelli et al., Nucl. Fus. 38 (1998) 649.
[9] S. Cappello, D. Biskamp, Nucl. Fus. 36 (1996) 571.
[10] P. Martin et al., Phys. Plasmas 7 (2000) 1984.
[11] P. Zanca, S. Martini, Plasma Phys. Contr. Fus. 41 (1999) 1251.
[12] L. Marrelli et al., J. Nucl. Mater. 266–269 (1999) 877.
[13] S. Cappello et al., in: Proceedings of the 26th EPS Conference On Controlled Fusion and Plasma Physics, Maastricht, The Netherlands, 14–18 June 1999, vol. 23J, p. 981.
[14] W. Ho, D.D. Schnack et al., Phys. Plasmas 2 (1995) 3407.
[15] R. Bartiromo, T. Bolzonella et al., Phys. Rev. Lett. 83 (1999) 1779.
[16] P. Zanca et al, these Proceedings.